Temperature- or Pressure-Induced Structure Changes of a Spin Crossover Fe(II) Complex; $[Fe(bpy)_2(NCS)_2]$

Michiko KONNO* and Mami MIKAMI-KIDO†
Department of Chemistry, Faculty of Science, Ochanomizu University, Ohtsuka, Bunkyo-ku, Tokyo 112
†Faculty of Liberal Arts, Information Science, Tohokugakuin University, Ichinazaka, Izumi-ku, Sendai, Miyagi 980
(Received April 16, 1990)

The crystal structures of polymorph II of diisothiocyanatobis(2,2′-bipyridine)iron(II), $[Fe(bpy)_2(NCS)_2]$, in the high- (298 K) and low-spin states (175, 110 K) were determined by an X-ray diffraction method. The crystal is orthorhombic, space group *Pcnb* and $Z=4$ over the entire temperature range. At 298 K, $a=13.2044$ (6), $b=16.4820$ (7), $c=10.1086$ (7) Å, $U=2200.0$ (2) Å^3, $D_c=1.462$ g cm^{-3} and at 110 K, $a=12.9842$ (9), $b=16.1067$ (12), $c=9.8938$ (8) Å, $U=2069.1$ (3) Å^3, $D_c=1.555$ g cm^{-3}. The structures were refined to $R=0.047$, 0.044, and 0.042 at 298, 175, and 110 K, respectively. The difference in the average Fe-N bond lengths between high- and low-spin states is 0.17 Å. The pressure dependence of the absorption spectra was also measured up to 8.5 GPa using a diamond anvil cell. These results indicate that with increasing pressure the high-spin state at 1 atm starts to change to the low-spin state at 0.3 GPa and that its low-spin state reverts again to the high-spin state at around 3.3 GPa.

Some iron(II) and iron(III) complexes exhibit spin transitions induced by temperature or pressure between different spin multiplicities.[1-4] Especially in iron(II) complexes, a drastic change was observed in the metal-ligand bond distance between high- and low-spin states[5-12] It is interesting to study the ligand field as well as the mechanism of spin transitions, since changes of ligand substituents, counter anions, solvent molecules, complex geometries, crystal forms, and states (solid or solution) cause various types of conversions between different spin states. Several theoretical models, a cooperative Jahn-Teller interaction,[13,14] the coupling to lattice vibrations[15] and the elastic interaction between high- and low-spin ions via an image pressure,[16] have been introduced in order to lead to a cooperative nature of the spin transitions. In order to understand the nature and the mechanism of spin transitions, it is necessary to investigate the difference among molecular geometries and molecular interactions between low- and high-spin states. The $[Fe(\alpha\text{-pic})_3]^{2+}$ system (α-pic=α-picolylamine) is one of the interesting ionic spin crossover complexes, since the effective magnetic moments depend on the nature of the counter anions or solvent molecules.[17-21] We determined the crystal structures of the $[Fe(\alpha\text{-pic})_3]Cl_2 \cdot EtOH$ compound at 298, 150, and 90 K and found that the average bond distance contracted by 0.18 Å upon making a transition from the high- to the low-spin state.[6,7] On the other hand, $[Fe(phen)_2(NCS)_2]$ (phen=1,10-phenanthroline) and $[Fe(bpy)_2(NCS)_2]$ complexes without solvent molecules are typical molecular spin crossover complexes showing discontinuous spin transitions; they have been investigated in detail by various means.[22-28] König et al.[24] reported on the magnetic susceptibility and Mössbauer spectra for three polymorphs of the $[Fe(bpy)_2(NCS)_2]$ complex as well as the preliminary results of the crystal structure ($R=0.19$—0.20) of polymorph II determined by a photographic method.[5] The difference in the Fe-N bond lengths (0.12 Å) between the high- and low-spin states observed by them appears to be small compared with those observed in other iron(II) spin crossover complexes.[6,7,11] We redetermined the crystal structures of the polymorph II of $[Fe(bpy)_2(NCS)_2]$ at 298, 175, and 110 K by a diffractometer method in order to gain more accurate information and to interpret the nature of the phase transitions and different magnetic behaviors between polymorphs I and II in the temperature range from 273 to 220 K. The change in the absorption spectra was also measured with increasing pressure up to 8.5 GPa in order to investigate the pressure effects for spin states.

Experimental

X-Ray Structure Analysis. Crystals were deep red and thin hexagonal (0 1 0) plates. The crystal specimens used for X-ray data collection were sealed in Lindemann-glass capillaries, since they are rather sensitive to air exposure. Oscillation and Weissenberg photographs taken at room temperature showed the crystal to be polymorph II. The crystal was cooled in a cold N_2 gas flow and kept constant at 175±1 and 110±1 K. The unit cell dimensions were refined by least-squares methods based on the values of 31, 19, and 16 reflections at 298, 175, and 110 K, respectively. The intensities were measured on an automated four-circle diffractometer with Mo$K\alpha$ radiation ($\lambda=0.71069$ Å) monochromated by graphite plate. Three standard reflections were recorded every fifty reflections. Though Lorentz and polarization corrections were applied, no correction was made for either absorption or extinction. Crystal data are summarized in Table 1.

The structure was solved by the conventional heavy-atom method. After several refinement cycles, difference syntheses showed an orientational disorder of an S atom on the

Table 1. Crystal Data of $[Fe(bpy)_2(NCS)_2]$

$[Fe^{II}(C_{10}H_8N_2)_2(NCS)_2]$, M.W. 484.38			
Orthorhombic, Space group *Pcnb*, $Z=4$			
	High-spin state	Low-spin state	
T/K	298	175	110
a/Å	13.2044(6)	13.0101(7)	12.9842(9)
b/Å	16.4820(7)	16.1384(11)	16.1067(12)
c/Å	10.1086(7)	9.9340(7)	9.8938(8)
U/Å^3	2200.0(2)	2085.8(2)	2069.1(3)
D_c/g cm^{-3}	1.462	1.543	1.555
μ(Mo $K\alpha$)/mm^{-1}	0.91	0.96	0.96
Crystal size/mm	0.40×0.35×0.18	0.33×0.27×0.15	
Scan method	ω-2θ	ω	ω
$2\theta_{max}$/°	60	55	55
Maximum repeating number	3	1	1
Independent reflections			
$[\|F_o\|\geq 3\sigma(\|F_o\|)]$	1379	1790	1835
R[a)]	0.047	0.044	0.042
R_2[a)]	0.055	0.052	0.053

a) $R=\sum\||F_o|-|F_c||/\sum|F_o|$. $R_2=\{\sum(|F_o|-|F_c|)^2/\sum|F_o|^2\}^{1/2}$.

NCS ligand at room temperature. Full-matrix least-squares refinements including a population of this disordered S atom were carried out by using a program called RADIEL.[29] In the low-spin state (175 and 110 K) the NCS group takes a regular position. Anisotropic thermal parameters were applied, except for H atoms and disordered S atom with a low population. Scatterring factors for Fe^{2+}, S, N, and C atoms were taken from International Tables for X-ray Crystallography[30] and for H atom from Stewart, Davidson, and Simpson.[31] The unit weight was used for all of the reflections. The final refinements for reflections corresponding to $|F_o|\geq 3\sigma(|F_o|)$ led to convergences of R=0.047, 0.044, and 0.042 at 298, 175, and 110 K, respectively. Final atomic parameters are given in Tables 2, 3, and 4.[32]

Table 2. Positional Parameters for Non-Hydrogen Atoms (×10^4, for Fe ×10^5, for S(2)×10^3) in the High-Spin State (298 K)

Atom	x	y	z	10^3U_{eq}[b)]/Å^2
Fe	0	25000	11320(9)	57 (0)
S(1)	−1129 (3)	1027 (5)	4934 (8)	87 (1)
N(1)	−557 (4)	1729 (3)	2551 (5)	85 (2)
N(2)	−240 (3)	1568 (2)	−367 (3)	55 (1)
N(3)	1476 (3)	1965 (2)	795 (4)	61 (1)
C(1)	−809 (4)	1433 (3)	3515 (5)	61 (2)
C(2)	−1143 (4)	1350 (3)	−858 (5)	68 (2)
C(3)	−1287 (5)	692 (4)	−1682 (5)	76 (2)
C(4)	−467 (5)	238 (4)	−2021 (6)	80 (2)
C(5)	466 (5)	443 (3)	−1529 (5)	71 (2)
C(6)	561 (3)	1108 (3)	−693 (4)	55 (2)
C(7)	1531 (3)	1354 (3)	−89 (5)	59 (2)
C(8)	2450 (4)	974 (4)	−381 (7)	89 (2)
C(9)	3312 (5)	1248 (5)	236 (8)	104 (3)
C(10)	3273 (5)	1856 (4)	1105 (8)	95 (3)
C(11)	2341 (5)	2202 (4)	1375 (7)	87 (2)
S(2)	−129 (2)	80 (2)	448 (3)	87 (6)[a)]

The populations for disordered atoms S are S(1)= 0.87(2) and S(2)=0.13(2).
a) Isotropic thermal parameter is given for S(2).
b) $U_{eq}=1/3\sum_i\sum_j U_{ij}a_i^*a_j^*\boldsymbol{a}_i\cdot\boldsymbol{a}_j$.

Table 3. Positional Prameters for Non-Hydrogen Atoms (×10^4, for Fe, S ×10^5) in the Low-Spin State (175 K)

Atom	x	y	z	10^3U_{eq}[b)]/Å^2
Fe	0	25000	9180(7)	21 (0)
S	−10576(8)	10402(7)	47729(11)	37 (0)
N(1)	−413 (3)	1740 (2)	2342 (3)	29 (1)
N(2)	−303 (2)	1635 (2)	−421 (3)	21 (1)
N(3)	1376 (2)	1994 (2)	812 (3)	23 (1)
C(1)	−679 (3)	1456 (2)	3347 (4)	24 (1)
C(2)	−1227 (3)	1454 (2)	−949 (4)	26 (1)
C(3)	−1392 (3)	783 (2)	−1789 (4)	29 (1)
C(4)	−579 (3)	272 (2)	−2107 (4)	30 (1)
C(5)	372 (3)	442 (2)	−1571 (4)	29 (1)
C(6)	491 (3)	1119 (2)	−712 (3)	22 (1)
C(7)	1460 (3)	1340 (2)	−49 (4)	23 (1)
C(8)	2385 (3)	934 (3)	−241 (5)	35 (1)
C(9)	3259 (3)	1207 (3)	412 (5)	37 (1)
C(10)	3177 (3)	1868 (3)	1273 (4)	35 (1)
C(11)	2227 (3)	2242 (2)	1463 (4)	31 (1)

Table 4. Positional Prameters for Non-Hydrogen Atoms (×10^4, for Fe, S ×10^5) in the Low-Spin State (110 K)

Atom	x	y	z	10^3U_{eq}[b)]/Å^2
Fe	0	25000	9032(6)	15 (0)
S	−10539(7)	10520(6)	47886(9)	26 (0)
N(1)	−415 (2)	1743 (2)	2335 (3)	21 (1)
N(2)	−306 (2)	1631 (2)	−430 (3)	15 (1)
N(3)	1376 (2)	1991 (2)	795 (3)	17 (1)
C(1)	−677 (3)	1462 (2)	3355 (3)	18 (1)
C(2)	−1236 (2)	1455 (2)	−962 (3)	19 (1)
C(3)	−1406 (3)	776 (2)	−1799 (3)	22 (1)
C(4)	−593 (3)	260 (2)	−2118 (3)	22 (1)
C(5)	364 (3)	426 (2)	−1573 (3)	20 (1)
C(6)	487 (2)	1113 (2)	−727 (3)	16 (1)
C(7)	1459 (2)	1334 (2)	−53 (3)	17 (1)
C(8)	2384 (3)	915 (2)	−244 (4)	24 (1)
C(9)	3255 (3)	1184 (2)	423 (4)	26 (1)
C(10)	3179 (3)	1864 (2)	1273 (4)	25 (1)
C(11)	2236 (3)	2238 (2)	1449 (4)	23 (1)

Absorption Spectra Measurements at High Pressures. The absorption spectra of a single crystal of [Fe(bpy)$_2$(NCS)$_2$] were measured under high pressure up to 8.5 GPa in the wavelength region 450—800 nm. A diamond anvil cell was used to generate high pressure.[33] Measurements were carried out by using a microscopic optical measurement system comprising a Nikon G250 spectrometer. A mixed solvent of pentane and isopentyl alcohol (1 : 1) was used for the pressure medium, since crystals are soluble to methyl or ethyl alcohol. A pressure calibration was made based on a shift of the ruby luminescence peaks. A He-Cd laser was employed for ruby excitation; its beam was 10 μm in diameter. Changes in the crystals were visually observed under the microscope and a TV monitor.

Results and Discussion

Crystal Structure. A projection of the crystal structure along the c-axis in the high-spin state is given in Fig. 1 and those along b-axis in both spin states are shown in Figs. 2(a) and (b). An iron atom of [Fe(bpy)$_2$(NCS)$_2$] molecule lies on a crystallographic two-fold axis along the c-axis and is octahedrally coordinated by two N atoms of isothiocyanate ligands in the cis-configuration and four N atoms of bidentate bipyridine ligands. The molecular symmetry of the structure remains the same in both high- and low-spin states. The general feature of the structure is the same as that reported by König and Watson.[5] However, remarkable structural changes according to the electronic configuration of two spin states including some orientational disorder of the NCS ligand were revealed from the present results. No crystallographic change was observed in the temperature range from 175 to 110 K, although a thermal anomaly at 145 K was observed in the heat-capacity measurements by Takahashi et al.,[34] besides a thermal anomaly at 213 K associated with the spin transition. The bond lengths and angles at 175 and 110 K are in good agreement within twice the esd's. They are listed in Table 5 together with those at 298 K. The average Fe-N value is 2.133 Å (298 K) in the high-spin state, while 1.962 (3) Å (175 K) and 1.959 (3) Å (110 K) in the low-spin state. The Fe-N bond difference of 0.17 Å between low- and high-spin states is consistent with that (0.18 Å) observed in [Fe(α-pic)$_3$]Cl$_2$·EtOH[6,7] and that (0.20 Å) observed between bis[hydrotris-(1-pyrazolyl)borato]iron(II) in the low-spin state and bis[hydrotris(3,5-dimethyl-1-pyrazolyl)borato]iron(II) in the high-spin state.[11] When looked into with more detail, the Fe-N bond distances were found to shorten by 0.207 Å for the bipyridine ligand and by 0.106 Å for the NCS ligand upon transition from the high- to low-spin state. The considerable Fe-N$_{(bpy)}$ shortening in the low-spin state appears to show large increase of back-donation of the dπ electron of the Fe atom to an empty π* orbital of the bipyridine ligand, as was observed in Fe-N$_{(py)}$ of [Fe(α-pic)$_3$]Cl$_2$·EtOH compound.[6,7]

The distortion on the FeN$_6$ core from an octahedron is smaller in the low-spin state than in the high-spin state. The twist angle between two triangles, which are defined by three N atoms on the planes perpendicular to the pseudo three-fold axis, is 45° in the high-spin state and 49° in the low-spin state. The tilt angle between two triangular faces is 8.2° at 298 K and 1.1° at 110 K. The N(1)-Fe-N(3) angle decreases from 100.4(2)° to 91.6(1)° upon going from the high- to the low-spin state, while N(1)-Fe-N(2′) and N(3)-Fe-N(3′) became closer to a linear configuration. Though the increases of the angle in N(2)-Fe-N(2′) and N(2)-Fe-N(3′) are in opposite directions, it seems to be related to a relative detachment of two bipyridine ligands with respect to each other in the low-spin state. This possibly occurs through a repulsion

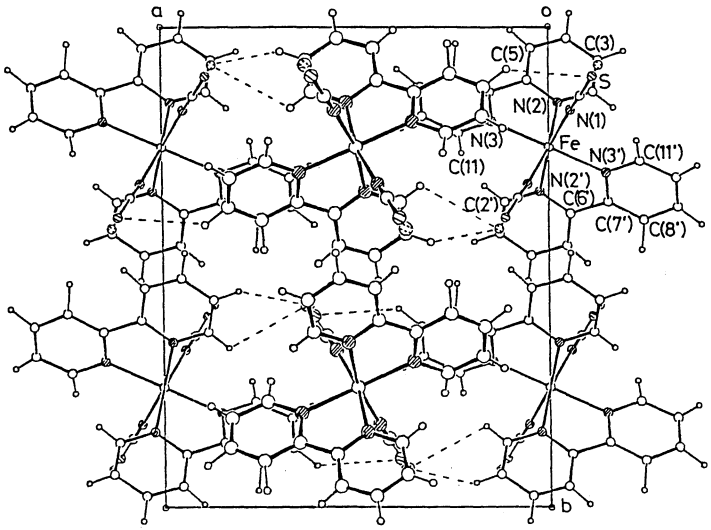

Fig. 1. A projection of [Fe(bpy)$_2$(NCS)$_2$] in the high-spin state (298 K) along c-axis.

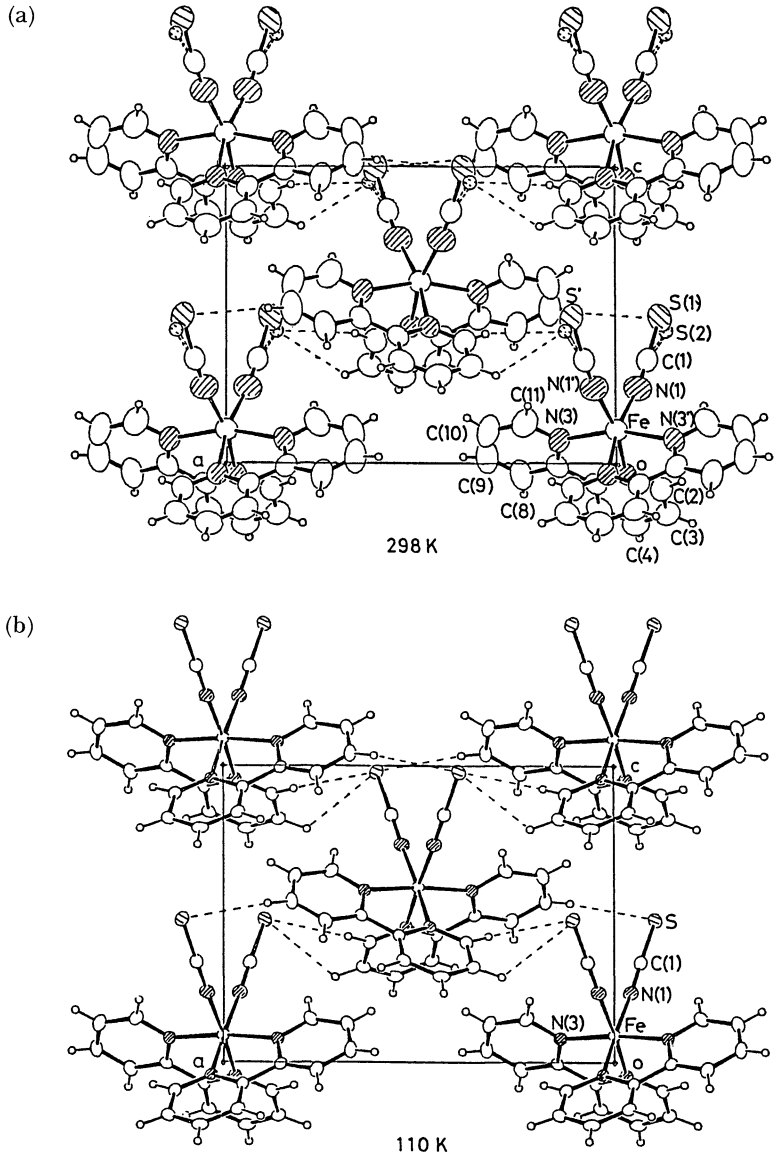

Fig. 2. Projections of $[Fe(bpy)_2(NCS)_2]$ along b-axis. (a) in the high-spin state (298 K), (b) in the low-spin state (110 K). Broken lines show short contacts between S and H atoms.

between an anti-bonding π^* orbital of bipyridine ligands, which has increased occupancy in the low-spin state due to the back-donation.

In the high-spin state the NCS ligands exhibit an orientational disorder of the S atoms at two sites with a population ratio ca. 7 : 1; in the low-spin state the NCS ligand takes a regular position. The S atom with a lower population contacts to H(3) with a short distance of 2.80(6) Å, indicating a weak hydrogen-bond between them. The interatomic distance between the S atom with a higher population and H(9) is 2.95(6) Å. On the other hand, in the low-spin state the NCS ligand takes the same arrangement as that of higher occupancy in the high-spin structure. A short contact between adjacent molecules is found between the S and H(9) with an interatomic distance of 2.89 (4) Å.

The bond distances and angles of the NCS ligand show that it resonates between the $Fe\text{-}N^-\text{=}C\text{=}S$ and $Fe\text{-}N\text{-}C\equiv S^-$ structures. The N(1)-C(1) bond distance is 1.139 (7) and 1.153 (4) Å at 298 and 110 K, respectively, indicating that the bond order is almost triple. The C(1)-S(1) bond length appears to be constant in both the high- and low-spin states and the average value of 1.638 Å seems to suggest that the bond order is between double and single, being much closer to the former. The larger occupation in the $Fe\text{-}N^-\text{=}C\text{=}S$ configuration brings about a larger deviation from 180° regarding the Fe-N-C bond angle owing to the sp^2 configuration of the N atom. The Fe-N(1)-C(1) angle is

Table 5. Bond Lengths and Bond Angles with esd's in Parentheses[a)]

T/K	298	175	110
(a) Bod lengths (l/Å)			
Fe-N(1)	2.053(5)	1.947(3)	1.945(3)
Fe-N(2)	2.181(4)	1.969(3)	1.964(2)
Fe-N(3)	2.166(4)	1.970(3)	1.969(3)
N(1)-C(1)	1.139(7)	1.152(5)	1.157(4)
C(1)-S	1.638(9)	1.642(4)	1.639(3)
N(2)-C(2)	1.341(6)	1.343(5)	1.348(4)
N(2)-C(6)	1.343(6)	1.357(4)	1.357(4)
N(3)-C(7)	1.349(6)	1.363(4)	1.355(4)
N(3)-C(11)	1.341(8)	1.343(5)	1.350(4)
C(2)-C(3)	1.380(8)	1.384(5)	1.389(5)
C(3)-C(4)	1.360(9)	1.379(6)	1.379(5)
C(4)-C(5)	1.371(9)	1.375(6)	1.381(5)
C(5)-C(6)	1.390(7)	1.395(5)	1.396(4)
C(6)-C(7)	1.475(6)	1.466(5)	1.471(4)
C(7)-C(8)	1.397(8)	1.384(5)	1.390(5)
C(8)-C(9)	1.374(9)	1.381(6)	1.380(5)
C(9)-C(10)	1.335(11)	1.375(6)	1.385(5)
C(10)-C(11)	1.383(9)	1.388(6)	1.376(5)
(b) Bond angles (ϕ/°)			
N(1)-Fe-N(2)	89.9(2)	89.4(1)	89.2(1)
N(1)-Fe-N(3)	100.4(2)	91.6(1)	91.7(1)
N(2)-Fe-N(3)	74.6(1)	81.5(1)	81.4(1)
N(1)-Fe-N(1′)	91.4(2)	86.8(1)	86.5(1)
N(1)-Fe-N(2′)	166.9(2)	173.1(1)	172.7(1)
N(1)-Fe-N(3′)	92.3(2)	92.8(1)	92.8(1)
N(2)-Fe-N(2′)	92.0(1)	95.0(1)	95.6(1)
N(2)-Fe-N(3′)	92.7(1)	94.3(1)	94.4(1)
N(3)-Fe-N(3′)	161.9(2)	173.9(1)	173.8(1)
Fe-N(1)-C(1)	165.3(4)	164.4(3)	164.4(3)
Fe-N(2)-C(2)	125.1(3)	126.7(2)	126.4(2)
Fe-N(2)-C(6)	117.0(3)	115.2(2)	115.5(2)
Fe-N(3)-C(7)	117.1(3)	115.3(2)	115.5(2)
Fe-N(3)-C(11)	125.4(4)	126.9(3)	127.0(2)
N(1)-C(1)-S	177.4(6)	179.3(4)	179.2(3)
C(6)-N(2)-C(2)	117.3(4)	117.7(3)	117.8(3)
N(2)-C(2)-C(3)	123.8(5)	123.0(3)	122.7(3)
C(2)-C(3)-C(4)	118.3(6)	119.1(4)	119.3(3)
C(3)-C(4)-C(5)	119.2(6)	118.8(4)	118.8(3)
C(4)-C(5)-C(6)	119.8(6)	119.5(4)	119.4(3)
C(5)-C(6)-N(2)	121.5(4)	121.7(3)	122.0(3)
N(2)-C(6)-C(7)	115.3(4)	114.2(3)	113.8(3)
C(11)-N(3)-C(7)	117.5(4)	117.8(3)	117.5(3)
N(3)-C(7)-C(8)	121.4(5)	121.5(3)	122.1(3)
C(7)-C(8)-C(9)	118.4(6)	120.0(4)	119.4(3)
C(8)-C(9)-C(10)	120.9(7)	118.5(4)	118.7(3)
C(9)-C(10)-C(11)	118.3(7)	119.3(4)	119.1(3)
C(10)-C(11)-N(3)	123.5(6)	122.8(4)	123.1(3)
N(3)-C(7)-C(6)	115.7(4)	113.6(3)	113.7(3)

a) Primed and unprimed atoms are related by a two-fold axis along the c-axis through the iron atom of the molecule.

165.3 (4)° at 298 K and 164.4 (3)° at 110 K, both of them shifting from linear coordination. A deviation of the M-N-C angle from 180° is usually found in octahedral coordination of the NCS ligand;[35,36] in tetrahedrally coordinated complex, however, $Co(NCS)_4Hg$, Co-N-C was observed to be linear.[37]

Two pyridine rings within a bipyridine ligand are slightly bent with respect to a five-membered ring in the opposite direction. As shown in Fig. 1, two pyridine rings of neighboring complexes related by a symmetry center are parallel and overlap each other with an interplanar distance of 3.503 Å (298 K) in the high-spin state and 3.495 Å (175 K) and 3.457 Å (110 K) in the low-spin state. There seems to be a charge-transfer interaction between these rings. The change of the interplanar distance upon a spin transition is small compared to the value expected from thermal expansion, suggesting that the occupation of the π^* orbital of the bipyridine ligand due to a back-donation in the low-spin state weakens the π-π^* charge transfer interaction between them.

Absorption Spectra at High Pressure. The absorption maximum was observed around 540 nm for the spectra of $[Fe(bpy)_2(NCS)_2]$ in the high-spin state at 1 atm; this was in good agreement with the results reported by Takahashi et al.[38] When the crystal was pressed to 0.4 GPa, the color darkened from deep red to dark red and the spectra exhibited a fine structure with two maxima at 545 and 570 nm. This indicates that the spin state had started to change from the high-spin to the low-spin state at 0.3 GPa, since the low-spin state spectra at 77 K/1 atm has two maxima at 538 and 595 nm.[38] The absorption edge of the spectra showed a remarkable red shift with increasing pressure and intensity saturation was observed in the wavelength region less than 600 nm. The intense visible absorption band around 600 nm can be assigned to a charge-transfer transition of t_{2g} to the π^* orbital in

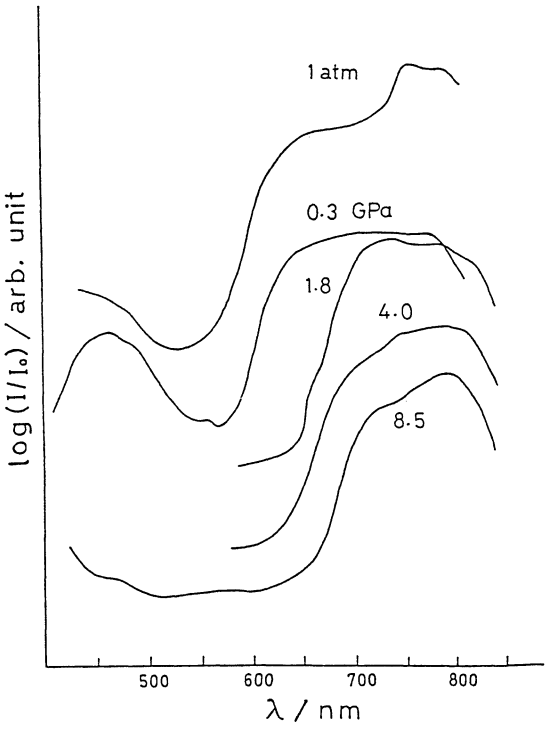

Fig. 3. Absorption spectra of $[Fe(bpy)_2(NCS)_2]$ under high pressure.

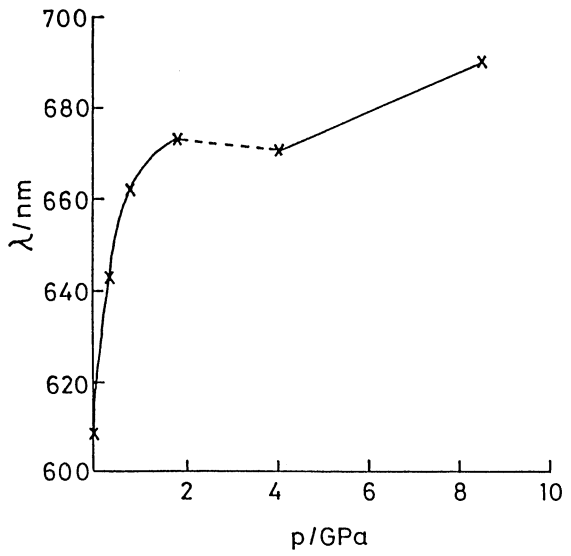

Fig. 4. Variation of absorption edge of $[Fe(bpy)_2(NCS)_2]$ under high pressure.

analogy with the case of $[Fe(phen)_2(NCS)_2]$.[23] At a pressure of 3.3 GPa a microscope observation showed that the crystal made a drastic change, displaying net-like boundaries on the surface, changing at every momemt, which seems to reflect something like a domain structure. Such movement continued for a few minutes; when it settled, the crystal color had lightened and once again became uniform. At that time, the absorption edge shifted back to a shorter wavelength region, as illustrated in Fig. 4. The iron(II) spin crossover complexes are known to exhibit pressure-induced spin transitions of the high- to the low-spin state under rather low pressure (up to ca. 2 GPa) and inversion of the low- to the high-spin state in the higher pressure range based on a ligand field calculation of the electronic states of both spin states.[3] The change around 3.3 GPa can be interpreted as being a latter conversion of the low- to the high-spin state. At 8.5 GPa, however, the spectra showed an entirely different feature from that of either the high- or the low-spin states. When the pressure was slowly reduced to 1 atm, the position of the small absorption maxima was slightly shifted by about 10 nm from the original position. One interpretation for this phenomenon is that the crystals changed from polymorph II to polymorph I by imposing pressure, since polymorph I has a larger density compared to polymorph II, their specific gravity being 1.482 and 1.462 $g\,cm^{-3}$, respectively. This can be understood structurally as being a small rotation of complex molecules, just like propellers facing in a certain direction systematically.

The authors are grateful to Professor Keisuke Suzuki and Jun Takahashi at the Faculty of Science of Kwansei Gakuin Univesity for the single crystals. Thanks are also due to Professor Takehiko Yagi of Institute for Solid State Physics, the University of Tokyo for all the facilities made available for measurements of the absorption spectra under high pressure. This work was carried out under the joint research in the Institute for Solid State Physics, the University of Tokyo.

References

1) H. A. Goodwin, *Coord. Chem. Rev.*, **18**, 293 (1976).
2) P. Gütlich, *Struct. Bonding*, **44**, 83 (1981).
3) D. C. Fisher and H. G. Drickamer, *J. Chem. Phys.*, **54**, 4825 (1971).
4) E. König, G. Ritter, W. Irler, and H. A. Goodwin, *J. Am. Chem. Soc.*, **102**, 4681 (1980).
5) E. König and K. J. Watson, *Chem. Phys. Lett.*, **6**, 457 (1970).
6) M. Mikami, M. Konno, and Y. Saito, *Chem. Phys. Lett.*, **63**, 566 (1979).
7) M. Mikami, M. Konno, and Y. Saito, *Acta Crystallogr, Sect. B*, **36**, 275 (1980).
8) A. M. Greenaway and E. Sinn, *J. Am. Chem. Soc.*, **100**, 8080 (1978).
9) A. M. Greenaway, C. J. O'Connor, A. Schrock, and E. Sinn, *Inorg. Chem.*, **18**, 2692 (1979).
10) B. A. Katz and C. E. Strouse, *J. Am. Chem. Soc.*, **101**, 6214 (1979).
11) J. D. Oliver, D. F. Mullica, B. B. Hutchinson, and W. O. Milligan, *Inorg. Chem.*, **19**, 165 (1980).
12) F. Cecconi, M. D. Vaira, S. Midollini, A. Orlandini, and L. Sacconi, *Inorg. Chem.*, **20**, 3423 (1981).
13) T. Kambara, *J. Chem. Phys.*, **70**, 4199 (1979).
14) T. Kambara, *J. Phys. Soc. Jpn.*, **49**, 1806 (1980).
15) R. Zimmermann and E. König, *J. Phys. Solids*, **38**, 779 (1977).
16) S. Ohnishi and S. Sugano, *J. Phys. C*, **14**, 39 (1981).
17) G. A. Renovitch and W. A. Baker, Jr., *J. Am. Chem. Soc.*, **89**, 6377 (1967).
18) M. Sorai, J. Ensling, and P. Gütlich, *Chem. Phys.*, **18**, 199 (1976).
19) M. Sorai, J. Ensling, K. M. Hasselbach, and P. Gütlich, *Chem. Phys.*, **20**, 197 (1977).
20) H. Koppen, E. W. Muller, C. P. Kohler, H. Spiering, E. Meissner, and P. Gütlich, *Chem. Phys. Lett.*, **91**, 348 (1982).
21) L. Wiehl, G. Kiel, C. P. Köhler, H. Spiering, and P. Gütlich, *Inorg. Chem.*, **25**, 1565 (1986).
22) W. A. Baker, Jr. and H. M. Bobonich, *Inorg. Chem.*, **3**, 1184 (1964).
23) E. König and K. Madeja, *Inorg. Chem.*, **6**, 48 (1967).
24) E. König, K. Madeja, and K. J. Watson, *J. Am. Chem. Soc.*, **90**, 1146 (1968).
25) J. H. Takemoto and B. Hutchinson, *Inorg. Chem.*, **12**, 705 (1973).
26) M. Sorai and S. Seki, *J. Phys. Chem. Solids*, **35**, 555 (1974).
27) P. G. Ganguli, P. Gütlich, E. W. Muller, and W. Irler, *J. Chem. Soc., Dalton Trans.*, **1981**, 441.
28) E. W. Muller, H. Spiering, and P. Gütlich, *Chem. Phys. Lett.*, **93**, 567 (1982).
29) P. Coppens, T. N. Guru-Row, P. Leung, E. D.

Stevens, P. J. Becker, and Y. W. Yang, *Acta Crystallogr., Sect. A*, **35**, 63 (1979).

30) "International Tables for X-Ray Crystallography," Kynoch Press, Birmingham (1974), Vol. IV, pp. 73—78.

31) R. F. Stewart, E. R. Davidson, and W. T. Simpson, *J. Chem. Phys.*, **42**, 3175 (1965).

32) Lists of structure factors, anisotropic thermal parameters for non-hydrogen atoms and positional parameters for hydrogen atoms are deposited as Document No. 9096 at the Office of the Editior of Bull. Chem. Soc. Jpn.

33) H. K. Mao and P. M. Bell, *Carnegie Inst. Washington, Year Book*, **77**, 904 (1978).

34) J. Takahashi, K. Suzuki, K. Tsuji, and S. Aeki, Molecular Structure Symposium of Japan, Kyoto, October 1981, Abstr., p. 470.

35) A. L. Beauchamp, L. Pazdernik, and R. Rivest, *Acta Crystallogr., Sect. B*, **32**, 650 (1976).

36) R. J. Restivo, J. Horney, and G. Ferguson, *J. Chem. Soc., Dalton Trans.*, **1976**, 514.

37) J. W. Jeffery and K. M. Rose, *Acta Crystallogr., Sect. B*, **24**, 653 (1968).

38) J. Takahashi, Y. Moriyama, K. Kashiwai, and K. Suzuki, The 43rd Annual Meeting of Chemical Society of Japan, Tokyo, April 1981, Abstr., Vol. I, p. 499.